COMPARATIVE STUDY OF OPTIMAL ACTIVE TWISTS FOR HELICOPTER ROTOR BLADES WITH C AND D-SPARS

[1]Andrey O. Kovalov, [2]Evgeny N. Barkanov, and [3]Sergey A. Gluhih

Institute of Materials and Structures, Riga Technical University
1 Kalku Str., Riga, LV-1658, Latvia
[1]e-mail: kovalovs@bf.rtu.lv
[2]e-mail: barkanov@latnet.lv
[3]e-mail: s_gluhih@inbox.lv

Keywords: macro-fibre composite (MFC), helicopter rotor blade, active twist, finite element method, optimisation.

Abstract: In time of helicopter flight, rotor blades produce significant vibration and noise as a result of variations in rotor blade aerodynamic loads with blade azimuth angle. Significant vibration and noise reduction can be achieved without the need for complex mechanisms in the rotating system using active twist control of helicopter rotor blades by an application of the macro-fiber composite (MFC) actuators. In this case MFC actuators are implemented in the form of active plies within the composite skin of the rotor blade with orientation at 45^0 to the blade axis to maximize the shear deformations in the laminated skin producing a distributed twisting moment along the blade. The present investigations are devoted to the comparative study of optimal active twist solutions obtained for the helicopter rotor blades with C and D-spars.
The baseline helicopter rotor blades consist of C or D-spars made of uni-directional GFRP, skin made of $+45^0/-45^0$ GFRP, foam core, MFC actuators embedded into the skin and balance weight. 3D finite element models of the rotor blades have been built by ANSYS, where rotor blade skin and spar thin parts are modelled by the linear layered structural shell elements SHELL99, and spar and foam by 3D 20-node structural solid elements SOLID186. Optimisation problems for the optimum placement of actuators in different helicopter rotor blades have been formulated on the results of parametric study using the finite element method. As the design parameters, the values characterising blades spar geometry, skin lay-up, position and size of actuators are chosen. The optimisation results have been obtained for two helicopter rotor blades and two possible applications of active materials

1. INTRODUCTION

In time of helicopter flight rotor blades produce significant vibration and noise as a result of variations in rotor blade aerodynamic loads with blade azimuth angle. For this reason future helicopters need to be improved with respect to environmental and public acceptance. Significant vibration and noise reduction can be achieved without the need for complex mechanisms in the rotating system using active twist control of helicopter rotor blades by an application of MFC actuators. In this case MFC actuators are implemented in the form of active plies within the composite skin of the rotor blade with orientation at 45^0 to the blade axis to maximize the shear deformations in the laminated skin producing a distributed twisting moment along the blade.
A number of theoretical and experimental studies have been performed to estimate an active twist of helicopter rotor blades required to effect noise and vibration reduction benefits, as well as to improve the overall performances of helicopters [1-5]. The design of an active

blade model based on a 1/6th Mach-scale Chinook CH-47D has been reviewed in paper [1]. The paper [2] presents investigations on the concept described as adaptive blade twist. It is based on a representative model in which the active part of the rotor blade is simplified with a thin-walled rectangular beam that is structurally equivalent to a model rotor blade of the Bo105 with a scaling factor 2.54. An evaluation of the performance of the active twist concept with respect to rotor dynamics, stability, aerodynamics, acoustics and piloting has been done in paper [3] for the Bo105 model rotor blade. The paper [4] presents the procedure and integrated tools for aeroelastic analysis of the Active Twist Rotor (ATR) with a rectangular blade and NACA0012 airfoil. The blades are modelled as beam elements by an original finite volume formulation for the analysis of non-linear, initially curved and twisted beams subjected to large displacements and rotations. This approach is extended to include the effects of embedded piezoelectric devices as actuators. An asymptotic formulation for analysing multi-cell composite helicopter rotor blades with integral anisotropic active plies was presented in paper [5] for the first time to design model scale ATR blades. The analysis derived in this paper consists of two parts: a linear 2D analysis of the cross-section and a geometrically non-linear (beam) analysis along the blade span. The present formulation has been validated on a 1/6th Mach-scale two-cell CH-47D active blade.
The models examined use simplified design parameters to reduce system complexity and to ease fabrication process. More modern blade design techniques and parameters are presented in papers [6-8] for the Advanced Active Twist Rotor (AATR). Recent achievements in helicopter and fixed wing aircraft applications of induced strain actuations are reviewed in paper [9], where two directions have been examined: distributed induced strain actuation resulting in a continuous twisting of the blade and discrete actuation of a servo aerodynamic control surface to generate localised aerodynamic forces. Recent investigations are devoted to the design of an active twist of helicopter rotor blades and only some to the active twist optimisation. So the capability to characterise numerically induced strain composite beam sections has been used in an optimisation problem to determine a design of the rotor blade in paper [10].
The objective of the present study is development of the methodology, based on the planning of experiments and response surface technique, for the optimal design of active rotor blades using MFC actuators to obtain high piezoelectric actuation forces and displacements with minimal actuator weight and energy applied. 3D structural static analysis with thermal load is carried out to characterise an active twist of the helicopter rotor blade. The optimisation results have been obtained for two helicopter rotor blades with C and D-spars and two possible applications of active materials

2. HELICOPTER ROTOR BLADES

The investigated helicopter rotor blades presented in Figure 1 is equipped with NACA23012 airfoil and has a rectangular shape with active part radius (R) 1.56 m and chord length (c) 0.121 m. The rotor blades consists of C-spar and D-spar made of unidirectional GFRP, skin made of $+45^0/-45^0$ GFRP, foam core, MFC actuators embedded into the skin and balance weight. MFC actuators consist of rectangular piezoceramic fibres embedded in an epoxy matrix and sandwiched between polyamide films that have attached interdigitated electrode patterns as shown in Figure 2. The interdigitated electrodes deliver the electric field required to activate the piezoelectric effect in the fibers and allows invoking the stronger longitudinal piezoelectric effect along the length of the fibers, which to maximize the shear deformations in the laminated skin producing a distributed twisting moment along the blade. The direction of piezoceramic fibres in MFC coincides with the direction of outside GFRP skin layers. Two design solutions are studied in connection with an application of active materials (Fig. 3). The

thickness of GFRP skin is t = 0.25·n mm, where n is the number of layers, and thickness of MFC layer is t_{MFC} = 0.3 mm. The material properties of the rotor blade components are

- GFRP
  E_x = 11.981 GPa, E_y = 11.981 GPa, E_z = 45.166 GPa,
  G_{xz} = 4.583 GPa, G_{yz} = 4.583 GPa, G_{xy} = 1.289 GPa,
  υ_{yz} = 0.238, υ_{xz} = 0.238, υ_{xy} = 0.325,
  ρ = 2008 kg/m^3
- foam (Rohacell 51 FX)
  E = 0.035 GPa, G = 0.014 GPa, υ = 0.25, ρ = 52 kg/m^3
- lead
  E = 13.790 GPa, G = 2.000 GPa, υ = 0.44, ρ = 11300 kg/m^3
- MFC
  E_x = 30.0 GPa, E_y = 15.5 GPa, E_z = 15.5 GPa,
  G_{xz} = 10.7 GPa, G_{yz} = 10.7 GPa, G_{xy} = 5.7 GPa,
  υ_{yz} = 0.4, υ_{xz} = 0.4, υ_{xy} = 0.35,
  d_{33} = 4.18×10^{-10} m/V, d_{32} = d_{31} = -1.98×10^{-10} m/V,
  ρ = 4700 kg/m^3

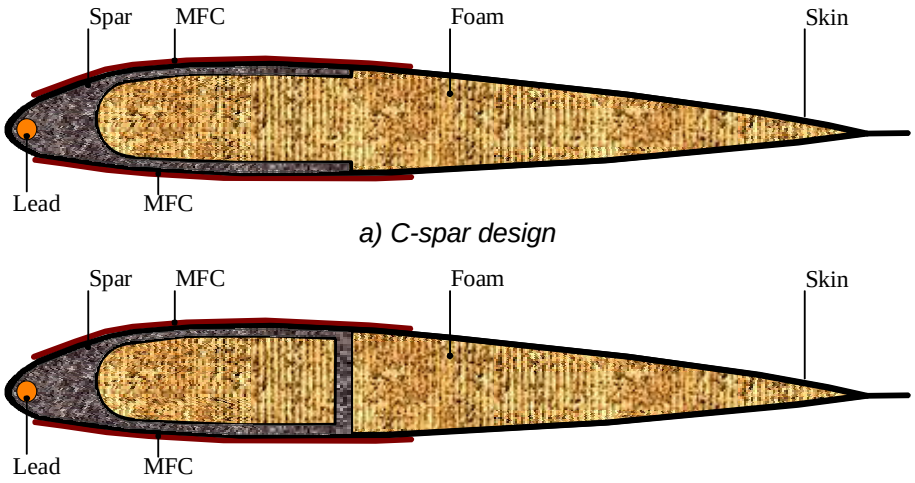

a) C-spar design

b) D-spar design

Figure 1. Cross-section of the helicopter rotor blades.

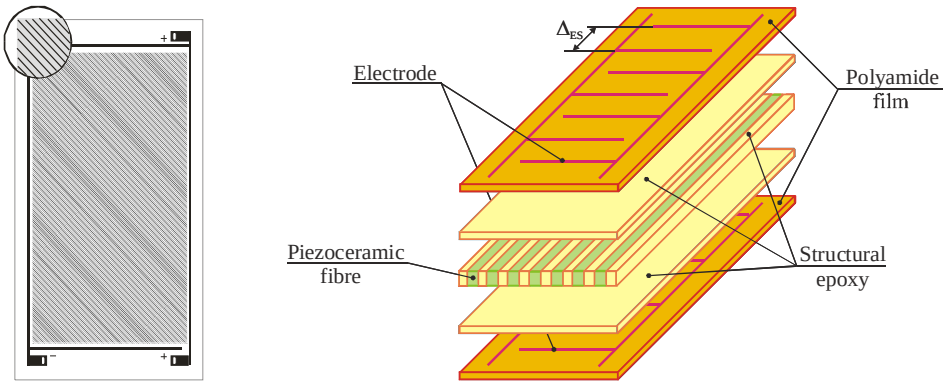

Figure 2. MFC actuator.

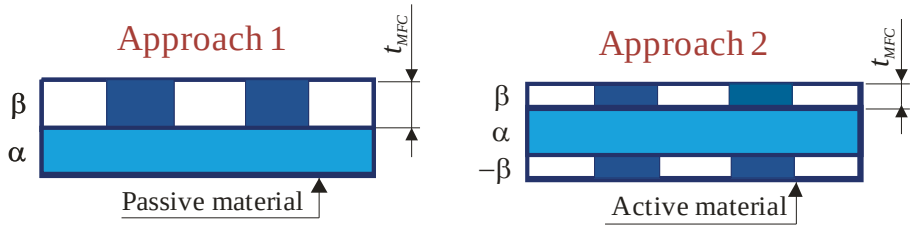

Figure 3. Application of active material.

3. FINITE ELEMENT ANALYSIS

The finite element method is used for helicopter rotor blade modelling and analysis in separate design points of the developed plan of experiments used in the optimisation process. 3D finite element model of the rotor blade is produced using ANSYS (Fig. 4), where rotor blade skin, web of spar and spar "moustaches" are modelled by the linear layered structural shell elements SHELL99, and spar and foam by 3D 20 node structural solid elements SOLID186. To avoid overstated stiffness of spar "moustaches", at least 8 finite elements should be taken to model this spar component. Some model simplification has been done, namely foam material has been removed from the rotor blade tile. This gives the possibility to decrease the dimension of the finite element model and to preserve a proportional mesh for the blade skin without accuracy loss for the obtained results. It is necessary to note that node offset option is applied for the joint skin-spar "moustaches" structure to preserve the rotor blade profile. In this case the finite element nodes are located at the top surface. Clamped boundary conditions are applied at one end of the rotor blade.

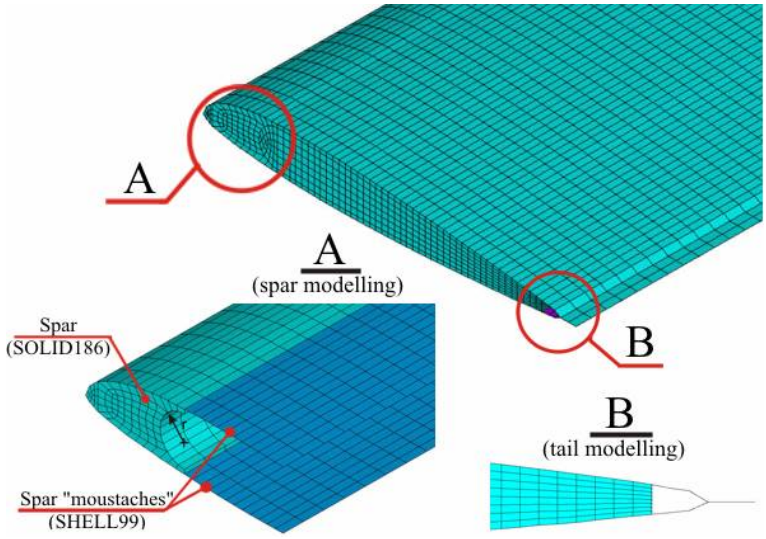

Figure 4. Finite element model of the helicopter rotor blade.

Thermal strain analogy between piezoelectric strains and thermally induced strains is used to model piezoelectric effects, when piezoelectric coefficients characterizing an actuator are introduced as thermal expansion coefficients determined by the following relationship

$$\alpha_{ij} = \frac{d_{ij}}{\Delta_{ES}} \tag{1}$$

where d_{ij} is the effective piezoelectric constant and Δ_{ES} is the electrode spacing (Fig. 2) taken as Δ_{ES} =0.5 mm. Structural static analysis with thermal load is carried out to determine a torsion angle of the rotor blade, static torsion analysis to determine the location of the elastic axis and modal analysis to determine the first torsion eigenfrequency of the rotor blade.
Before formulation of optimisation problem, a parametric study has been carried out with the purpose to decrease the number of design parameters and by this way to increase the accuracy of obtained optimal results. In this connection an influence of possible design parameters (spar "moustaches" thickness and length, web thickness, spar circular fitting, skin thickness, MFC chord-wise length and gluing variant, voltage) on behaviour functions (torsion angle, location of centre of gravity and elastic axis, mass of cross-section, strains and first torsion eigenfrequency) has been investigated [10,11,12]. The smallest influence has been shown by spar length. For this reason this parameter have been excluded from the set of design parameters used in optimisation problem for the optimum placement of actuators in helicopter rotor blades.

4. OPTIMAL DESIGN

Due to large dimension of the numerical problem to be solved, non-direct optimisation technique should be applied, since an application of direct minimisation algorithms and multiple finite element analysis is too expensive from a computational point of view. For this reason an optimisation methodology is developed employing the method of experimental design and response surface technique (Fig. 5). It is necessary to note, that in each of these stages, it is possible to solve the problem by different methods.

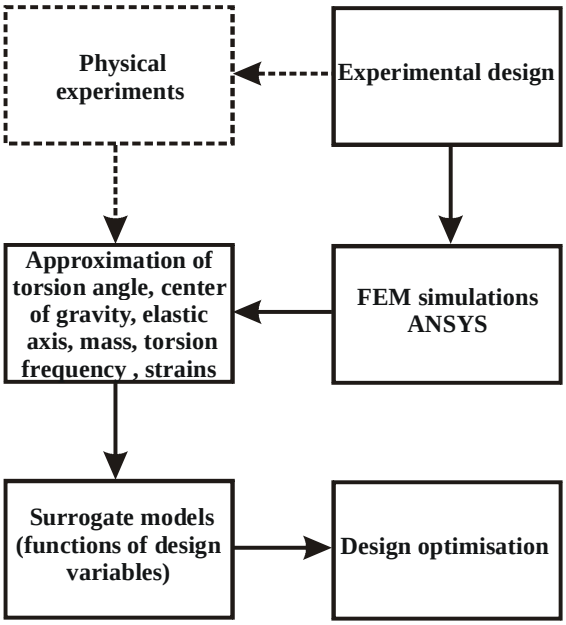

Figure 5. Optimisation procedure.

4.1. Formulation of Optimisation Problem

An optimisation problem for the optimum placement of actuators in the helicopter rotor blade (Fig. 6) has been formulated based on the results of parametric study and taking into account the producers requirements:

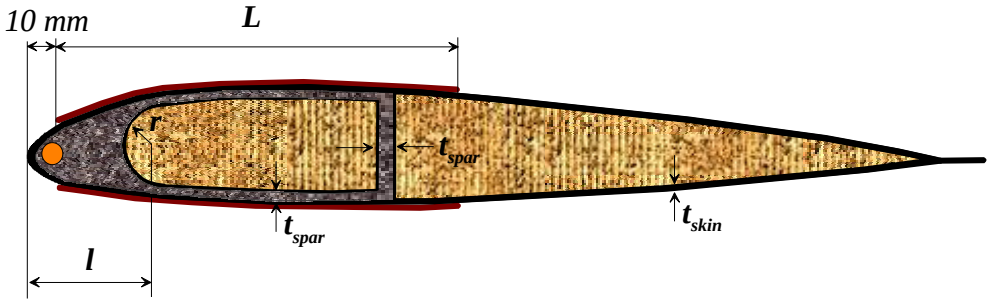

a) C-spar design

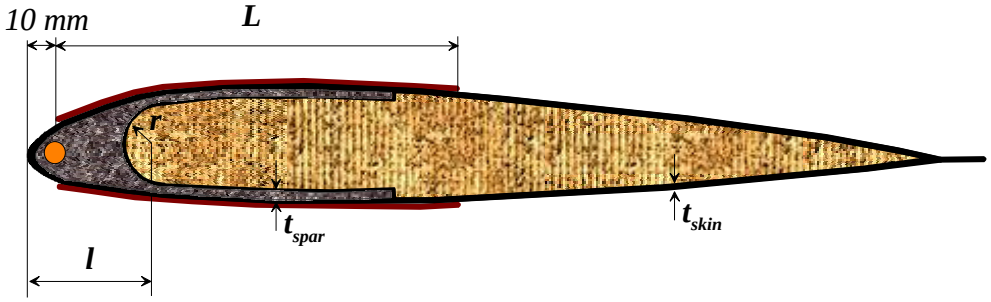

b) D-spar design

Figure 6. Design parameters.

Objective function: $\varphi(X) \Rightarrow MAX$

Design parameters: $\{X\} = \{l, t_{skin}, t_{spar}, L\}$

$16 \le l \le 24$

$0.25 \le t_{skin} \le 1.25$

$0.50 \le t_{spar} \le 2.50$

$16 \le L \le 100$

Constraints:

$22 \le y_{cg} \le 30$

$10 \le y_{ea} \le 25$

$m \le 1.35$

$f_{T1} \ge 59.1$

$\varepsilon_{max} \le 4000/k_s$

where φ - torsion angle (°), l - spar circular fitting (mm), t_{skin} - skin thickness (mm), t_{spar} - spar thickness (mm), L - MFC chord-wise length (mm), y_{cg} - location of the centre of gravity (%), y_{ea} - location of the elastic axis (%), m - mass of cross-section (kg/m), f_{T1}- first torsion eigenfrequency (Hz) and ε_{max} - admissible strains (μstrain) with the safety factor k_s=1.4. It is necessary to note that skin thickness is examined as discrete value design parameter with the following step $\Delta t_{(+45/-45)}$ = 0.25 mm. Voltage is constant 1000 V.

4.2. Experimental Design and FEM Simulations

The plan of experiment [13] is formulated for 4 design parameters and 30 experiments. Subsequently, in the points of the plan of experiments structural static analysis with thermal load is carried out to determine the torsion angles and strains arising in the helicopter rotor blade, and modal analysis to determine it first torsion eigenfrequency. As additional parameters the location of the centre of gravity and the rotor blade mass are found from the finite element model. Determination of the elastic axis location is more complicated problem and requires solution of additional static torsion problem with two forces applied independently from both sides of sought elastic centre [14].

4.2. Response Surfaces

In the present approach the form of the equation of regression is unknown in advance [15]. There are two requirements for the equation of regression: accuracy and reliability. Accuracy is characterised as a minimum of standard deviation of the table data from the values given by the equation of regression. Increasing the number of terms in the equation of regression it is possible to obtain a complete agreement between the table data and values given by the equation of regression. However, it is necessary to note that prediction in the intervals between the table points cannot be as accurate. For an improvement of prediction, it is necessary to decrease the distance between the points of experiments by increasing the number of experiments or by decreasing the domain of factors. Reliability of the equation of regression can be characterised by the affirmation that standard deviations for the table points and for any other points are approximately the same. Obviously the reliability is greater for a smaller number of terms of the equation of regression.
The equation of regression can be written in the following form

$$y = \sum_{i=1}^{p} A_i f_i(x_j) \tag{2}$$

where A_i are the coefficients of the equation of regression, $f_i(x_j)$ are the functions from the bank of simple functions $\theta_1, \theta_2, \ldots, \theta_m$, which are assume as,

$$\theta_m(x_j) = \prod_{i=1}^{s} x_j^{\xi_{mi}} \tag{3}$$

where ξ_{mi} is a positive or negative integer including zero. Synthesis of the equation from the bank of simple functions is carried out in two stages: selection of perspective functions from the bank and then step-by-step elimination of the selected functions.
In the first stage, all variants are tested with the least square method and the function, which leads to the minimum of the sum of deviations, is chosen for each variant. In the second stage, the elimination is carried out using the standard deviation

$$\sigma_0 = \sqrt{\frac{S}{k-p+1}} \quad , \quad \sigma = \sqrt{\frac{1}{k-1}\sum_{i=1}^{k}\left(y_i - \frac{1}{k}\sum_{j=1}^{k} y_j\right)^2} \tag{4}$$

or correlation coefficient

$$c = \left(1 - \frac{\sigma}{\sigma_0}\right) * 100\% \tag{5}$$

where k is the number of experimental points, p is the number of selected perspective functions and S is the minimum sum of deviations. It is more convenient to characterise the accuracy of the equation of regression by the correlation coefficient (Fig. 7). If insignificant functions are eliminated from the equation of regression, the reduction of the correlation coefficient is negligible. If in the equation of regression only significant functions are

presented, elimination of one of them leads to important decrease of the correlation coefficient.

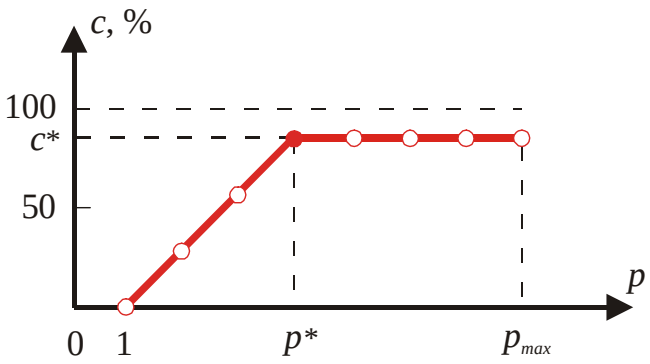

Figure 7. Diagram of elimination for the correlation coefficient.

Response surfaces for all behaviour functions have been obtained with the correlation coefficients around 90% and higher. They have been verified by the finite element solutions in points different from the points taken in the plan of experiments. Results of verification are presented in Figure 8.

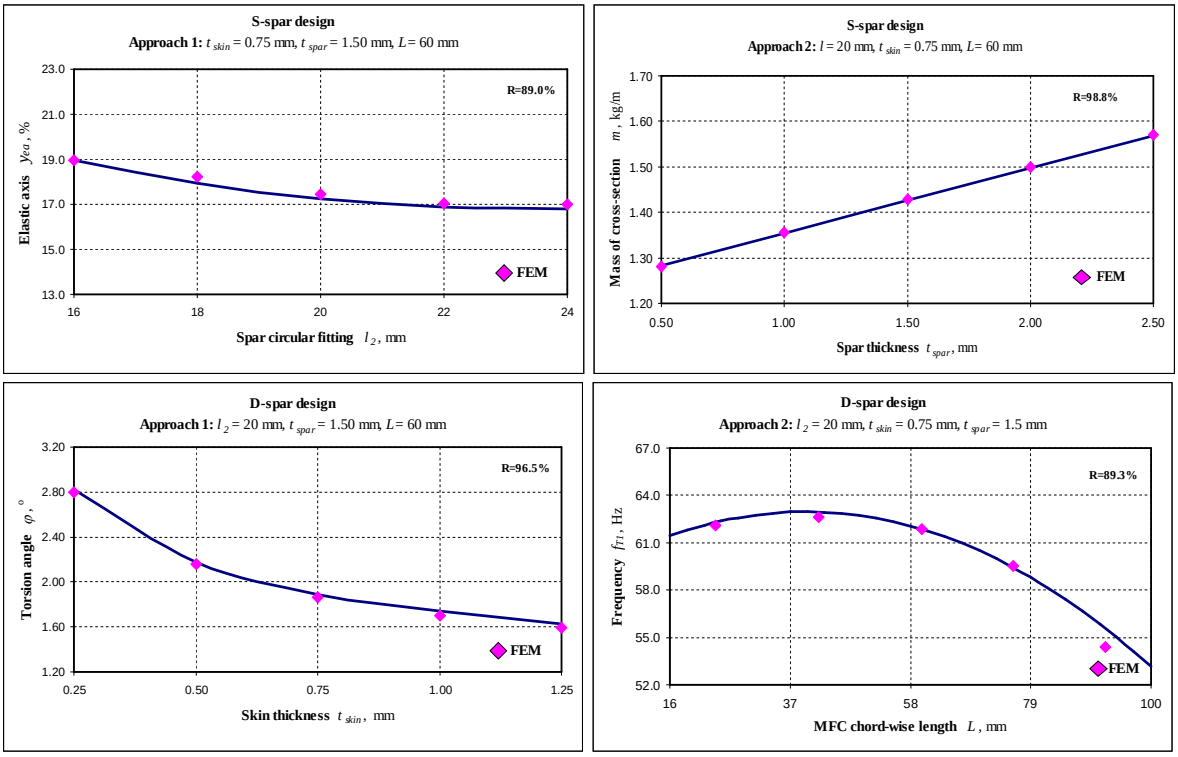

Figure 8. Finite element verification of response surfaces.

4.3. Optimisation Results

Non-linear optimisation problem is executed by the random search method [16] using the obtained response surfaces. In the first stage the design problem has been solved with the purpose to obtain maximal torsion angle. Optimisation results for first approach of C and D-spar design are given in Table 1, showing that the results for C and D-spar design almost are the same. Difference between results is 2.5 %. But the minimal distance between location of

the centre of gravity and elastic axis for C-spar is 10.2% and for D-spar is 7.6%. In this case D-spar is effective on 25.5%. Optimisation results for second approach is presented in Table 2, where it is seen that this approach more effective in compare with first approach for the maximal torsion angle more than 25%. Difference between results of torsion angles for second approach are 2.4 %. However, the minimal distance between location of the centre of gravity and elastic axis for C-spar is 13.2% and for D-spar is 11.3 %. Effectiveness of D-spar for second approach is only 14.4%.
From these results it is seen that the D-spar is always more effective than S-spar in compare for the minimal distance between location of the centre of gravity and elastic axis. But result for maximal torsion angle is the same.

TABLE 1

Optimal solutions for a maximal torsion angle Approach1.

Approach 1	Design parameters				Constraints				Objective function	Effecti-veness
	l mm	t_{skin} mm	t_{spar} mm	L mm	y_{cg} %	y_{ea} %	m kg/m	f_{T1} Hz	φ °	φ/R °/m
C-spar design										
Response surfaces	24	0.25	0.50	91	26.5	16.3	0.99	59.15	3.91	2.51
FEM	24	0.25	0.50	90	26.7	16.6	0.99	57.90	3.88	2.49
Δ %	-	-	-	-	0.7	1.8	0.0	2.1	0.7	0.8
D-spar design										
Response surfaces	16	0.25	1.00	89	29.7	22.1	0.96	59.15	4.01	2.57
FEM	16	0.25	1.00	88	29.4	21.9	0.95	58.10	4.04	2.59
Δ %	-	-	-	-	1.0	0.9	1.0	1.8	0.7	0.8

TABLE 2

Optimal solutions for a maximal torsion angle Approach2.

Approach 2	Design parameters				Constraints				Objective function	Effecti-veness
	l mm	t_{skin} mm	t_{spar} mm	L mm	y_{cg} %	y_{ea} %	m kg/m	f_{T1} Hz	φ °	φ/R °/m
C-spar design										
Response surfaces	16	0.25	1.50	77	28.9	15.7	1.16	59.30	5.52	3.54
FEM	16	0.25	1.50	76	29.2	16.0	1.14	59.82	5.56	3.56
Δ %	-	-	-	-	1.0	1.8	1.7	0.9	0.7	0.6
D-spar design										
Response surfaces	22	0.25	0.50	82	29.4	18.1	1.20	59.77	5.39	3.46
FEM	22	0.25	0.50	82	29.0	17.7	1.23	58.88	5.39	3.46
Δ %	-	-	-	-	1.4	2.3	2.5	1.5	0.0	0.0

5. CONCLUSION

The methodology based on the planning of experiments and response surface technique has been developed for the optimum placements of actuators in helicopter rotor blades. To describe the behaviour of twisted rotor blade, the finite element method has been applied in the sample points of experimental design. For this purpose the structural static analysis with thermal load, static torsion analysis and modal analysis using 3D finite element models have been developed using ANSYS. In the finite element modelling more attention should be paid to the convergence of the finite element results due to the complexity of the structure

analysed and large differences (factors greater than 1000) between Young's and shear module of different rotor blade components. Approximations of the original functions for behaviour constrains and objective function have been obtained using low order polynomials with some eliminated points. Minimisation problems have been solved for two approaches of C and D-spar by the method of random search employing the approximating functions instead of original functions.

From optimisation results it is seen that the D-spar and S-spar has approximately the same results of maximal angle for two approaches. However, the minimal distance of the centre of gravity and elastic axis more effective for D-spar, especially for first approach.

From approximation functions designer can find compromise between necessary solutions using obtained optimal results.

ACKNOWLEDGEMENTS

This work was supported by the European Commission under FRAMEWORK6 program, contract No. AIP3-CT-2003-502773, integrated project "Integration of technologies in support of a passenger and environmentally friendly helicopter" (FRIENDCOPTER).

REFERENCES

[1] J. P. Rodgers and N. W. Hagood, Design, Manufacture and Testing of an Integral Twist-Actuated Rotor Blade, Proc. 8th Int. Adaptive Structures and Technology Conf., 1997.

[2] A. Büter and E. Breitbach, Adaptive Blade Twist – Calculations and Experimental Results, Aerospace Science Technology, vol. 4, 2000, pp. 309-319.

[3] J. Riemenschneider, S. Keye, P. Wierach and H. M. des Rochettes, Overview of the Common DLD/ONERA Project "Active Twist Blade" (ATB), Proc. 30th European Rotorcraft Forum, 2004, pp. 22.1-22.9.

[4] G. L. Ghiringhelli, P. Masarati and P. Mantegazza, Analysis of an Actively Twisted Rotor by Multibody Global Modelling, Composite Structures, vol. 52/1, pp. 113-122, 2001.

[5] C. E. S. Cesnik and S. Shin, On the Modelling of Integrally Actuated Helicopter Blades, Int. J. Solids and Structures, vol. 38, 2001, pp. 1765-1789.

[6] M. K. Sekula, M. L. Wilbur and W. T. Yeager, Aerodynamic Design Study of an Advanced Active Twist Rotor, Proc. American Helicopter Society, 4th Decennial Specialist's Aeromechanics Conf., 2004.

[7] M. K. Sekula, M. L. Wilbur and W. T. Yeager, Structural Design Study of an Advanced Active Twist Rotor, Proc. 61st Annual Forum of the American Helicopter Society, 2005.

[8] M. L. Wilbur and M. K. Sekula, The Effect of Tip Geometry on Active-Twist Rotor Response, Proc. 61st Annual Forum of the American Helicopter Society, 2005.

[9] V. Giurgiutiu, Active-Materials Induced-Strain Actuation for Aeroelastic Vibration Control, The Shock and Vibration Digest, vol. 32/5, 2000, pp. 355-368.

[10] P. Masarati, M. Morandini, J. Riemenschneider, P. Wierach, S. Gluhih and E. Barkanov, Optimal Design of an Active Twist 1:2.5 Scale Rotor Blade, Proc. 31st European Rotorcraft Forum, 2005, pp. 37.1-37.14.

[11] A. Kovalovs, S. Gluhih, E. Barkanov, P. Masarati, M. Morandini, D. Muffo and J. Riemenschneider, Active Twist Design of Helicopter Rotor Blades, Mechanics of Composite Materials, submitted for publication, 2007.

[12] A. Kovalovs, E. Barkanov, S. Gluhih, Active twist of model rotor blades with D-spar design, Transport, 2007, XXII-1, pp. 38-44..

[13] E. Barkanov, R. Rikards, A. Chate, Numerical optimization of sandwich and laminated composite structures, Computer Aided Optimum Design of Structures, 1995, pp. 311-318.

[14] I. Obrazcov, Structural mechanics of aircraft, 1986. (In Russian)
[15] R. Rikards, Elaboration of Optimal Design Models for Objects from Data of Experiments, Proc. IUTAM Symp., Elsevier Science Publishers, Amsterdam, 1992, pp. 148-162.
[16] A. Janushevskis, T. Akinfiev, J. Auzins and A. Boyko, A Comparative Analysis of Global Search Procedures, in Proc. Estonian Acad. Sci. Eng., vol. 10/4, 2004, pp. 236-250.